Coupled-cluster calculations of matrix elements and ionization energies of low-lying states in sodium

Sten Salomonson and Anders Ynnerman
Department of Physics, University of Göteborg and Chalmers University of Technology, S-412 96 Göteborg, Sweden
(Received 9 July 1990)

Accurate nonrelativistic calculations of ionization energies and hyperfine structures for the 3*s* and the 3*p* states, and of the dipole transition 3*s*-3*p*, are presented for Na, using wave functions obtained in the coupled-cluster approach including single and double excitations (CCSD). Agreement with experimental results is at the percent level, corresponding to an error in the correlation contribution of approximately 5%. Certain three-body cluster contributions to the 3*s* ionization energy and the 3*s* hyperfine structure are evaluated and are found to account for the main part of the discrepancies between the values obtained from CCSD calculations and the experimental results.

I. INTRODUCTION

During the last two decades atomic many-body theory has proved to be successful in calculating atomic properties such as ionization energies and hyperfine structures. In 1975 Garpman *et al.*[1] performed the first complete third-order calculation of the hyperfine structure, using an effective-operator form of perturbation theory. Since then many sodium hyperfine calculations have been presented (see, e.g., Lindgren, Lindgren, and Mårtensson,[2] Grundevik *et al.*,[3] Lindgren,[4] and Johnson, Idrees, and Sapirstein[5]). Ionization energies and dipole oscillator strengths for the sodium atom have recently been calculated in the multiconfiguration Hartree-Fock (MCHF) approach by Froese-Fischer,[6] and by Johnson, Idrees, and Sapirstein,[5] using relativistic many-body perturbation theory.

The coupled-cluster approach to the many-body problem has shown to be a very fruitful method, and in a recent paper by Mårtensson-Pendrill and Ynnerman[7] a general approach to the evaluation of matrix elements in the coupled-cluster theory is presented and applied to the lithium atom, using coupled-cluster singles and doubles (CCSD) wave functions obtained from the "pair program" by Salomonson and Öster.[8] The hyperfine structure has for a long period of time been the natural testing ground for atomic many-body theory, and not many calculations have included other external perturbations than the hyperfine operator. However, it is now easy, using a computer code based on the above-mentioned general formalism of Mårtensson-Pendrill and Ynnerman,[7] to treat other types of one-particle perturbations, such as the dipole operator and the field shift operator.[9]

Sodium calculations are natural extensions of previous calculations on lithium, and provide good tests for the new formalism and computer code. In this paper we present calculations of the hyperfine structure of the 3*s* and 3*p* states and the 3*s*-3*p* dipole transition. Also the ionization energy of the 3*s* state is calculated. A class of three-particle effects that are not included in the CCSD approximation is evaluated for this state, to yield a deeper understanding of the importance of such effects in the alkali-metal atoms.

II. WAVE FUNCTIONS AND MATRIX ELEMENTS IN THE COUPLED-CLUSTER SINGLE- AND DOUBLE-EXCITATION APPROXIMATION

In the coupled-cluster approach the exact wave function $|\Psi\rangle$ is written in terms of a zeroth-order wave function $|\Psi^0\rangle$ as

$$|\Psi\rangle=\{\exp(S)\}|\Psi^0\rangle\ , \tag{1}$$

where the curly brackets denote normal ordering and S the cluster operator, which can be divided into one-, two-, . . . , n-particle excitations:

$$S=S_1+S_2+S_3+\cdots\ . \tag{2}$$

An introduction to the coupled-cluster theory was given, e.g., by Bishop and Kümmel.[10] In this section a complete treatment of single and double excitations, using intermediate normalization (IN), as described by Lindgren and Morrison,[11] Salomonson and Öster,[8] or Lindgren and Salomonson[12] is used. In Fig. 1 the graphical representation of the cluster operator, truncated after double excitations, is shown.

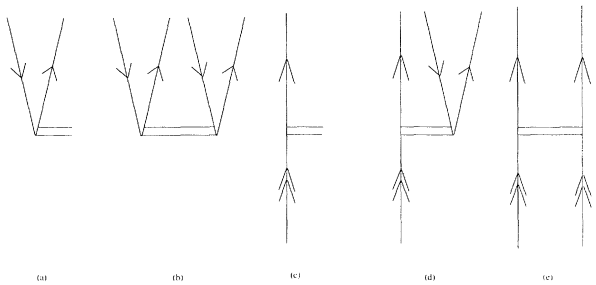

FIG. 1. Diagrammatic representation of the cluster operator limited to single and double excitations. Down- (up-) going lines denote core (excited) orbitals and double arrows denote valence orbitals. The horizontal double lines indicate that several perturbation interactions are included in the self-consistent solution of the cluster equations.

The effect of the single-particle clusters can be treated as corrections to the occupied orbitals

$$|\delta a\rangle = \sum_r S_a^r |r\rangle \ , \tag{3}$$

and the double excitations are treated by the use of pair functions as described by Mårtensson[13] and Lindgren and Morrison.[11] The pair functions are written in terms of the cluster operator and the product functions of the excited orbitals as

$$|U_{ab}\rangle = \sum_{r,s} S_{ab}^{rs} |rs\rangle \ . \tag{4}$$

The orbital corrections $|\delta a\rangle$ as well as the pair functions $|U_{ab}\rangle$ describing double excitations were obtained as sums over a discretized numerical basis set using the methods described by Salomonson and Öster.[14]

In order to evaluate the matrix elements of a one-particle operator

$$\frac{\langle \Psi_f^0 | \{\exp(S_f^\dagger)\} O \{\exp(S_i)\} | \Psi_i^0 \rangle}{\langle \Psi_f^0 | \{\exp(S_f^\dagger)\} \{\exp(S_f)\} | \Psi_f^0 \rangle^{1/2} \langle \Psi_i^0 | \{\exp(S_i^\dagger)\} \{\exp(S_i)\} | \Psi_i^0 \rangle^{1/2}} \ , \tag{5}$$

the procedure described by Mårtensson-Pendrill and Ynnerman[7] is followed. The graphical equivalents of the leading terms of Eq. (5) are shown in Fig. 2.

The unperturbed wave functions for the valence orbitals were obtained in the Hartree-Fock potential of the Na^+ core. Single excitations then enter first in second order and describe modifications of the orbitals to approximate Brueckner orbitals, through central-field effects and polarization. The core is thus made aware of the valence electron, and thereby the valence orbital is caused to contract. The correction of the valence orbital was found to give one of the major contributions to the $\langle r^{-3} \rangle$ hyperfine parameters.

The diagrams in Figs. 3(c) and 3(d) are evaluated through repeated use of the two-particle cluster and iterated until self-consistency is reached. The well-known "random-phase approximation" (see, e.g., Amusia and Cherepkov[15]) is then to be considered as a well-defined subset of Fig. 2(d).

The diagrams in Figs. 2(e) and 2(f) are obtained by evaluating the matrix element of the external perturbation between two core-valence pair excitations, where the interaction occurs on an excited (core) line, respectively. In Figs. 2(g) and 2(h) both pair excitations involve two core electrons, and overlaps between these pair functions and the modified valence orbital from Fig. 3(a) are used in the evaluation.

In the next section we investigate the addition of the S_3 contributions to the cluster operator.

III. THREE-PARTICLE EFFECTS

When using the coupled-cluster formalism based on intermediate normalization, the S_3 cluster contributes already in third order for the ionization energies. Some typical diagrams of this kind are shown in Fig. 4.

Within this group of diagrams there are large cancellations. For example, in the diagram in Fig. 4(a) the valence electron can interact with either a core or a virtual electron line giving contributions of opposite sign, which would cancel exactly if the valence electron were completely outside the core. The diagrams in Figs. 4(b) and 4(c) show the asymmetry of the formulation based on IN, since their Hermitian conjugates are already included in the CCSD approximation. In a Hermitian formulation[16] the diagrams in Fig. 4 are all included together with their Hermitian conjugates in the CCSD scheme. Diagrams of the type in Fig. 4 have been evaluated, and found to give very small contributions for Na, by Blundell *et al.*[17] and are in their work denoted by $E_{\text{extra}}^{(3)}$.[18]

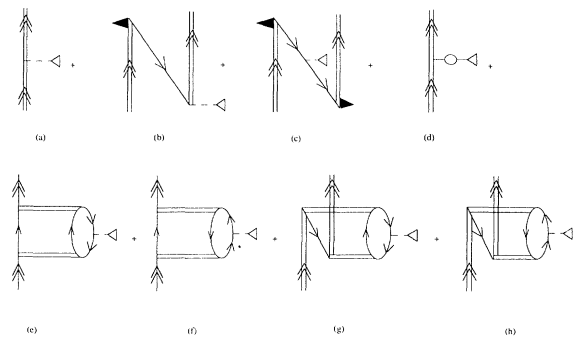

FIG. 2. Diagrammatic representation, using the definitions in Fig. 3, of the leading terms of the numerator in Eq. (5). The dotted horizontal line with the open triangle denotes the external perturbation. Exchange variants and Hermitian conjugate diagrams are not shown.

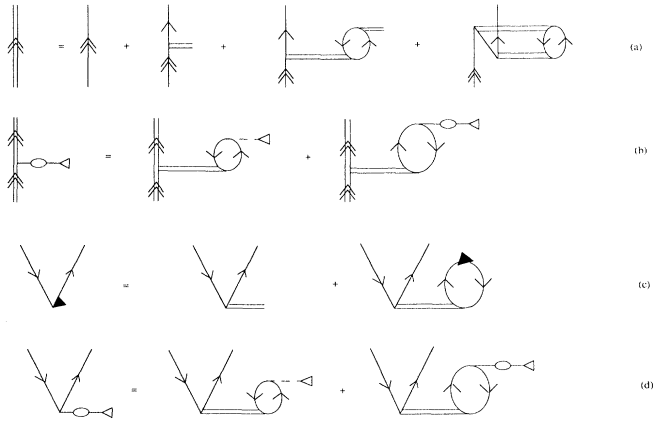

FIG. 3. Graphical definitions of the symbols used in Fig. 2. On the right-hand sides of (b), (c), and (d) the Hermitian conjugates of the left-hand side of (c) and (d) are used.

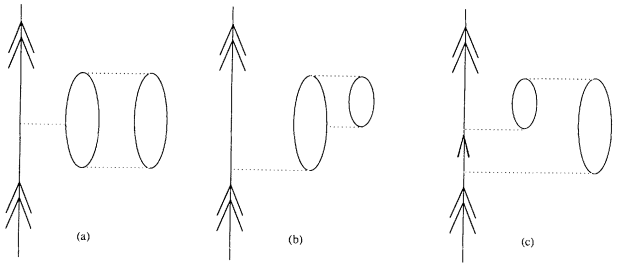

FIG. 4. Typical third-order diagrams based on the S_3 cluster in intermediate normalization. In a Hermitian formulation these diagrams are already accounted for by the S_1 and S_2 clusters.

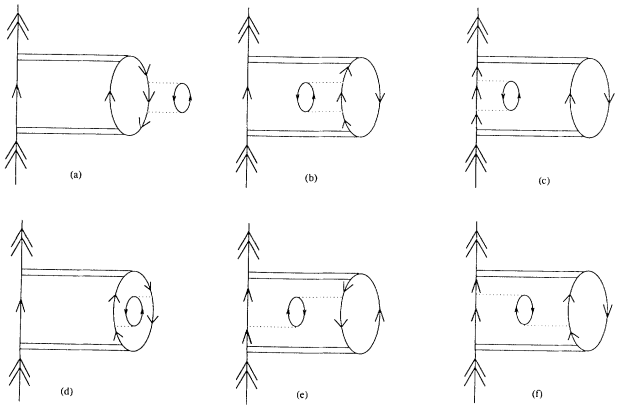

FIG. 5. Three-particle diagrams evaluated for the 3s state in Na. These diagrams cannot be included in a CCSD approximation even if a Hermitian formulation is used.

Genuine three-particle effects that cannot be included in the Hermitian formulation of the coupled-cluster equations are thus likely to account for the missing part of the correlation energy for Na. These diagrams occur first in fourth order. We have evaluated a certain class of these diagrams, shown in Fig. 5. The diagrams in Figs. 5(a)–5(c) originate from the second-order direct correlation energy diagram by the insertion of a Brueckner-like correction on the internal lines, and the diagrams in Figs. 5(d)–5(f) from the insertion of a screened Coulomb interaction, which is also known to be important.

IV. THE HYPERFINE-STRUCTURE OPERATORS

The magnetic hyperfine structure arises from an interaction between the magnetic multipole fields caused by the electrons and the magnetic moments of the nucleus with nonzero spin. In the relativistic case, the dipole interaction has a relatively simple form (see, e.g., Armstrong[19] or Lindgren and Rosén[20]). Using SI units it is

$$h^{\mathrm{mhfs}}=-2i\frac{\mu_0}{4\pi}\frac{\mu_B}{\alpha a_0}\frac{1}{r^2}(\boldsymbol{\alpha}\cdot\mathbf{1C}^1)\cdot\boldsymbol{\mu}_I\ , \tag{6}$$

where the nuclear magnetic moment is $\boldsymbol{\mu}_I=g_I\mathbf{I}$, $g_I=1.477\,49$ for ^{23}Na, and μ_0, μ_B, and α are the permeability of vacuum, the Bohr magneton, and the fine-structure constant, respectively. [In Hartree atomic units the constant in Eq. (6) is $-2i\alpha/2$.] The components of the $\mathbf{C}^k$ tensor are related to the spherical harmonics as $C^k_q=\sqrt{4\pi/(2k+1)}\,Y^k_q$, $\boldsymbol{\alpha}$ is related to the Pauli spin matrices as

$$\boldsymbol{\alpha}=\begin{bmatrix}0 & \boldsymbol{\sigma}\\ \boldsymbol{\sigma} & 0\end{bmatrix},$$

and $\mathbf{l}$ denotes the orbital angular momentum. The nonrelativistic equivalent operator to Eq. (6) is

$$\frac{\mu_0\mu_B}{2\pi}\left[\frac{1}{r^3}-\frac{\sqrt{10}(\mathbf{sC}^2)^1}{r^3}+\frac{2\mathbf{s}}{3}\frac{\delta(r)}{r^2}\right]\cdot\boldsymbol{\mu}_I\ . \tag{7}$$

In the central-field approximation only the valence electrons contribute to the hyperfine interaction. The effect of correlation can be included by the use of an effective operator acting only on the valence electrons. For a single valence electron, this effective operator can be written in an exact way as

$$\frac{\mu_0\mu_B}{2\pi}[1\langle r^{-3}\rangle_{01}-\sqrt{10}(\mathbf{sC}^2)^1\langle r^{-3}\rangle_{12}+\mathbf{s}\langle r^{-3}\rangle_{10}]\cdot\boldsymbol{\mu}_I\ , \tag{8}$$

using three different $\langle r^{-3}\rangle_{\kappa k}$ parameters, where κ and k denote the rank in spin and orbital space, respectively. These parameters are obtained directly in a nonrelativistic calculation. Results of experimental hyperfine-structure measurements are usually given in terms of A factors. For a single electron outside a closed shell, the expressions[21,20]

$$A(j_<)=Cg_I\frac{1}{2l+1}\left[(2l+2)\langle r^{-3}\rangle_{01}+\frac{2l+2}{2l-1}\langle r^{-3}\rangle_{12}-\langle r^{-3}\rangle_{10}\right], \tag{9a}$$

$$A(j_>)=Cg_I\frac{1}{2l+1}\left[2l\langle r^{-3}\rangle_{01}-\frac{2l}{2l+3}\langle r^{-3}\rangle_{12}+\langle r^{-3}\rangle_{10}\right], \tag{9b}$$

$$A(j_<,j_>)=Cg_I\frac{1}{2l+1}(\langle r^{-3}\rangle_{01}-\tfrac{1}{2}\langle r^{-3}\rangle_{12}-\langle r^{-3}\rangle_{10}) \tag{9c}$$

relate the A factors (in MHz) to the $\langle r^{-3}\rangle$ parameters (in Hartree atomic units), with $C=95.521\,32=\alpha^2(2cR_\infty)(m_e/M_p)(\mu_e/\mu_B)$, where the factor (μ_e/μ_B) accounts for the anomalous magnetic moment of the electron. The finite nuclear mass which changes the $\langle r^{-3}\rangle$ parameters by a factor of $(1-m/M)^3$ was found to give negligible corrections for Na.

If both the electron and the nucleus have a total angular momentum ≥ 1 then also the electric quadrupole fields may contribute through the interaction $e^2\mathbf{C}^2\cdot\mathbf{Q}/8\pi\epsilon_0 r^3$, where $\mathbf{Q}$ is the nuclear electric quadrupole moment. Experimental results are traditionally quoted in terms of B factors (in MHz) related to the quadrupole parameter (in atomic units) as

$$B_j=D\frac{2j-1}{2j+2}\langle r^{-3}\rangle_{nl}Q\ , \tag{10}$$

where the conversion factor is $D=234.9647=2cR_\infty\times 10^{-28}m^2/a_0^2$, and Q is given in barn. Knowledge of an experimental B factor thus makes it possible to extract a value for Q, if a theoretical $\langle r^{-3}\rangle$ parameter is available.

V. THE ELECTRIC DIPOLE OPERATOR

The oscillator strength between an initial state i and a final state f is determined by the matrix element of the electric dipole operator. The dipole operator, given in Hartree atomic units, is[22]

$$P_q^1=\sum_i^N r_q^{(1)}(i)=\sum_i^N r_i C_q^{(1)}(i)\ . \tag{11}$$

The weighted oscillator strength gf is then obtained from the expressions

$$gf=\tfrac{2}{3}(\Delta E)S\ , \tag{12}$$

$$S=|\langle f\|P^{(1)}\|i\rangle|^2\ , \tag{13}$$

where ΔE is the energy difference between the initial and the final states. Assuming that S is evaluated using uncoupled ls functions, for an s-p transition, thereby implicitly summing over all possible j values, the oscillator strengths for $s_{1/2}-p_{1/2}$ and $s_{1/2}-p_{3/2}$ transitions are obtained as

$$f(s_{1/2}-p_{1/2})=\tfrac{1}{3}gf(s-p)\ , \tag{14}$$

$$f(s_{1/2}-p_{3/2})=\tfrac{2}{3}gf(s-p)\ . \tag{15}$$

VI. RESULTS AND DISCUSSION

The orbital corrections as well as the individual pair functions, which were expanded in partial waves, each associated with a function of the radii for the two electrons, were obtained from the pair program by Salomonson and Öster[8,14] as sums over a discretized numerical basis set. In this work, logarithmic grids with $r=\exp(x)/Z$ were used with equal spacing in x. Here Z denotes the nuclear charge. Two different grids with 81 and 91 points in the range $\exp(-8)/Z-\exp(6)/Z$ were used. The results from the two grids were extrapolated to account for the finite number of grid points used. In practice it was found that the extrapolated values coincided to the required accuracy with the results using a single grid. In the multipole expansion of the Coulomb interaction, k values were limited to 4, 5, 6, and 7. Contributions from higher k values were then extrapolated assuming a k^{-4} dependence.

As can be seen in Table I, there is a 6% discrepancy between the CCSD and the experimental value for the correlation energy of the 3s state. Both relativistic correlation effects and the diagrams in Fig. 4, denoted by $E^{(3)}_{\text{extra}}$, give small total contributions. The three-particle diagrams shown in Fig. 5 were then evaluated, as de-

TABLE I. Ionization energies for the Na 3s state in microhartrees (1 μhartree = 10^{-6} a.u.).

Dirac-Fock	182 033	
Correlation		
CCSD		6428
Relativistic correlation[b]		30
$E^{(3)}_{\text{extra}}$[a]		69
Fig. 5(a)		306
Fig. 5(b)		107
Fig. 5(c)		68
Fig. 5(d)		−129
Fig. 5(e)		−77
Fig. 5(f)		38
Total	188 873	6840
Experimental	188 858	6825

[a]Blundell (Ref. 17), with k and l limited to 4 in the spherical expansion of the pair functions.
[b]Comparison between second-order relativistic and nonrelativistic calculations.

TABLE II. A diagrammatic breakdown of the contributions to the 3s hyperfine constant A (using $g_I=1.477\,49$ for ^{23}Na), and the reduced dipole matrix element for the 3s-3p transition in Na, with k in the multipole expansion of the Coulomb interaction restricted to 7.

Diagram	$A\langle 3s_{1/2}\rangle$ (MHz)	$\langle 3p\|\mathbf{r}\|3s\rangle$ (a.u.)
Hartree-Fock (HF)	616.64	4.525 80
Fig. 2(a)−HF	95.145	−0.126 58
Fig. 2(b)	7.622	−3.55[−4]
Fig. 2(c)	0.086	2.37[−6]
Fig. 2(d)	130.042	−0.054 54
"First order"		
Fig. 2(d)	3.765	0.001 97
"Higher orders"		
Fig. 2(e)	0.928	−8.04[−5]
Fig. 2(f)	9.550	0.003 45
Fig. 2(g)	4.396	1.42[−4]
Fig. 2(h)	1.698	−6.11[−5]
Normalization contribution	−3.007	−0.010 38
Fig. 6	5.0	
Relativistic corrections	11.9	
Total	883.7	4.339 37

TABLE III. Magnetic dipole and electric quadrupole hyperfine constants for $3s$ and $3p$ of Na, and reduced matrix elements of the dipole transition $3s$-$3p$ in Na.

	Magnetic dipole A (MHz)			Electric quadrupole B/Q (MHz/b)		$\langle 3p\|\|\mathbf{r}\|\|3s\rangle$ (a.u.)
Term	$^2S_{1/2}$	$^2P_{1/2}$	$^2P_{3/2}$	$^2P_{1/2,3/2}$	$^2P_{3/2}$	
HF	616.641	62.9717	12.5944	3.9357	15.7259	4.525 80
Coupled-cluster contributions						
$k_{max}=4$	249.635	29.1919	5.6576	1.1228	10.3070	−0.185 66
$k_{max}=5$	249.962	29.1822	5.6592	1.1164	10.3000	−0.186 11
$k_{max}=6$	250.110	29.1764	5.6596	1.1135	10.2968	−0.186 32
$k_{max}=7$	250.188	29.1729	5.6598	1.1120	10.2951	−0.186 43
extrapolated	250.3	29.16	5.660	1.108	10.29	−0.1868
Fig. 6	5.0					
Relativistic correlations[a]	11.9	0.88	0.064	0.020	0.12	−0.0056
Total	883.8	93.02	18.318	5.064	26.14	4.3334
Experiment	885.82[b]	94.3(2)[c]	18.65(10)[d]			
Lindgren[e]	870.5	92.89	18.56			
Johnson, Idrees, and Sapirstein[f]	860.90	91.40	19.80			4.342
Froese-Fischer[g]						4.3305
Grundevik *et al.*[h]		92.38	18.52	4.84	27.88	
Lundberg, Mårtensson, and Svanberg[i]	873.0					

[a]The relativistic corrections for the hyperfine structure were obtained from Rosen and Lindgren (Ref. 23), and for the dipole transition the ratio between the Hartree-Fock value and the Dirac-Fock value was used as correction factor.
[b]Logan and Kusch (Ref. 24)
[c]Hartman (Ref. 25)
[d]Schönberner and Zimmerman (Ref. 26).
[e]Reference 4.
[f]Reference 5.
[g]Nonrelativistic value, Ref. 6.
[h]Reference 3.
[i]Reference 27.

scribed above, using pair functions obtained in the CCSD approximation for the top and the bottom interaction in each diagram. The total result, for the $3s$ state, is then found to agree to within 0.3% with the experimental value. For the $3p$ state we have no value for the $E^{(3)}_{extra}$ diagrams, and a full calculation will be presented in a future paper.

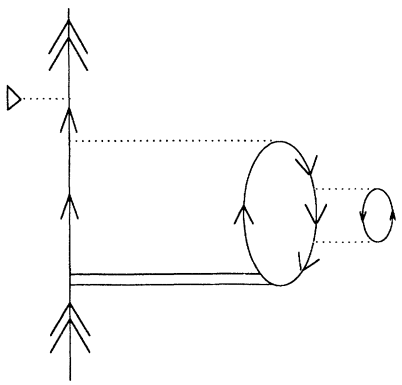

FIG. 6. Three-particle diagram evaluated for the $3s$ hyperfine structure.

In Table II a diagrammatic breakdown, for $k=7$, of the contributions to the $3s$ hyperfine structure and the reduced matrix element of the dipole operator is shown. In Table III all the final extrapolated values are given.

For the $3s$ hyperfine interaction, the discrepancy between experimental and the present result is less than 1%. The three-particle diagram shown in Fig. 6 gives a surprisingly large contribution, and the final result when this is added deviates from the experimental one by only 0.2%. Adding the hyperfine perturbation on the valence lines in all the diagrams in Fig. 5 will give diagrams similar to the one shown in Fig. 6. It is our intention to include all these possible diagrams in a future calculation. It is also noted that the dominating correction to the Hartree-Fock value arises from the diagram in Fig. 2(d), in which the core orbitals are spin polarized by the valence electron, causing the contact interaction to increase. It is therefore plausible that the insertion of such effects on the hyperfine interaction in Fig. 6 will give significant contributions.

The coupled-cluster contributions to the hyperfine structure of the $^3P_{1/2}$ and $^3P_{3/2}$ states are approximately $\frac{1}{3}$ of the total values. A comparison with experimental results shows small discrepancies of the order of 1%. The calculations by Lindgren,[4] using the methods de-

TABLE IV. Dipole oscillator strengths for the resonance lines in Na.

	$f(3s_{1/2}-3p_{1/2})$	$f(3s_{1/2}-3p_{3/2})$
Present	$\frac{1}{3}(0.9671)$	$\frac{2}{3}(0.9682)$
Johnson, Idrees, and Sapirstein[a]	$\frac{1}{3}(0.9709)$	$\frac{2}{3}(0.9717)$
Froese-Fischer[b]	$\frac{1}{3}(0.9707)$	$\frac{2}{3}(0.9717)$
Froese-Fischer[c]	$\frac{1}{3}(0.9682)$	$\frac{2}{3}(0.9692)$
Experiment	$\frac{1}{3}(0.9536\pm0.0016)$[d]	$\frac{2}{3}(0.9465\pm0.0023)$[e]

[a] Reference 5.
[b] Reference 6.
[c] Froese-Fischer (Ref. 6) multiplied with the square root of the ratio between the Dirac-Fock and Hartree-Fock values for the dipole matrix elements to account for relativistic effects.
[d] Laser-excited decay, Gaupp, Kuske, and Andrä (Ref. 30).
[e] Gawlik *et al.* (Ref. 31).

scribed in Ref. 28, are found to agree to within 1% with the present calculation. The difference for the $^3P_{1/2}$ state is as small as 0.2%.

As mentioned above, it is also possible for the $3p$ valence electron to interact with the nucleus through an electric quadrupole field. Knowledge of the experimental value of the B factor,[29] 2.90(21) MHz, and the calculated ratio B/Q enables an estimation of the nuclear quadrupole moment. Use of the value in Table II gives $Q=111$ mb.

The average value of $A(^3P_{1/2})$ and $A(^3P_{3/2})$ eliminates the effect of the contact parameter, as can be seen in Eqs. 9(a) and 9(b). The value obtained from Lindgren[4] then agrees to within 0.01% with the present calculation, while the experimental value is approximately 1% larger.

In the second column of Table II the contributions to the reduced matrix element of the dipole operator are shown. The coupled-cluster corrections to the Hartree-Fock value are very small, approximately 4% of the total value, and the experimental value differs by approximately 1% from the value presented here. To facilitate a direct comparison with experimental oscillator strengths, the observed energy differences are used in Eq. (12) to obtain the values in Table IV. These values agree very well with the MCHF calculation by Froese-Fischer.[6] As can be seen in Table IV, all the theoretical results are approximately 2% above the experimental value. Even though this may seem to be a small discrepancy, we must remember that the total effect of the correlation is only of the order of 10%, implying that, if the experimental results are correct, only 80% of the correlation is accounted for. A similar situation was found for the lithium atom.[7,18] Different theoretical approaches, neglecting different effects, seem to give similar results. Further experimental and theoretical investigation is certainly required to find the cause of this discrepancy.

The relativistic corrections to the hyperfine parameters were obtained by multiplying the total values with the correction factors for the valence electron given by Rosén and Lindgren.[23] For the dipole transition, the correction factor was obtained by taking the ratio between the DF and the HF value. It would, however, be desirable to perform a fully relativistic calculation, since the correction factors used may not be accurate for the coupled-cluster contributions. Such a program is presently being developed within our group at Chalmers University of Technology.

ACKNOWLEDGMENTS

Ingvar Lindgren is greatly acknowledged for letting us use his unpublished results from previous Na calculations and for constant support and fruitful discussions. We are grateful to Ann-Marie Mårtensson-Pendrill for many stimulating discussions and comments on the manuscript and for her expertise on coupled-cluster matrix element calculations. This work has greatly benefited from discussions with Steve Blundell about his Na calculations and particularly his evaluation of the $E^{(3)}_{\text{extra}}$ diagrams. This work would have been impossible without the use of the CCSD pair program developed in collaboration with Per Öster. Financial support by the Swedish Natural Science Research Council (NFR) is gratefully acknowledged.

[1] S. Garpman, I. Lindgren, J. Lindgren, and J. Morrison, J. Phys. Rev. A **11**, 758 (1975).
[2] I. Lindgren, J. Lindgren, and A.-M. Mårtensson, Z. Phys. A **279**, 113 (1976).
[3] P. Grundevik, H. Lundberg, A.-M. Mårtensson, K. Nyström, and S. Svanberg, J. Phys. B **12**, 2645 (1979).
[4] I. Lindgren (unpublished).
[5] W. R. Johnson, M. Idrees, and J. Sapirstein, Phys. Rev. A **35**, 3218 (1987).
[6] C. Froese-Fischer, Nucl. Instrum. Methods B **31**, 265 (1988).
[7] A.-M. Mårtensson-Pendrill and A. Ynnerman, Phys. Scr. **41**, 329 (1990).
[8] S. Salomonson and P. Öster, Phys. Rev. A **41**, 4670 (1990).
[9] A.-M. Mårtensson-Pendrill, L. Pendrill, S. Salomonson, A. Ynnerman, and H. Warston, J. Phys. B **23**, 1749 (1990).
[10] R. F. Bishop and H. G. Kümmel, Physics Today **40** (3), 52 (1987).
[11] I. Lindgren and J. Morrison, *Atomic Many-Body Theory*, 2nd ed., Vol. 3 of *Springer Series on Atoms + Plasmas*, edited by G. Ecker, P. Lambropoulos, and H. Walther (Springer-Verlag, Berlin, 1986).
[12] I. Lindgren and S. Salomonson, Phys. Scr. **21**, 335 (1980).
[13] A.-M. Mårtensson, J. Phys. B **12**, 3995 (1979).
[14] S. Salomonson and P. Öster, Phys. Rev. A **40**, 5548 (1989).
[15] M. Ya Amusia and N. A. Cherepkov, At. Phys. **5**, 47 (1975).
[16] I. Lindgren, Nucl. Instrum. Methods B **31**, 102 (1988) and J. Phys. B (to be published).
[17] S. Blundell (private communication).
[18] S. Blundell, W. R. Johnson, Z. W. Liu, and J. Sapirstein, J. Phys. Rev. A **40**, 2233 (1989).
[19] L. Armstrong, Jr., *Theory of the Hyperfine Structure of Free Atoms* (Wiley-Interscience, New York, 1971).

[20]I. Lindgren and A. Rosén, At. Phys. **4**, 150 (1974).
[21]S. Garpman, I. Lindgren, J. Lindgren, and J. Morrison, Z. Phys. A **276**, 167 (1976).
[22]R. D. Cowan, *The Theory of Atomic Structure and Spectra*, Los Alamos Series in Basic and Applied Sciences, edited by D. H. Sharp and L. M. Simmons, Jr. (University of California Press, Berkeley, 1981).
[23]A. Rosén and I. Lindgren, Phys. Scr. **6**, 109 (1972).
[24]R. A. Logan and P. Kusch, Phys. Rev. **81**, 323 (1970).
[25]W. Hartman, Z. Phys. **240**, 323 (1970).
[26]D. Schönberner and D. Zimmerman, Z. Phys. **216**, 172 (1968).
[27]H. Lundberg, A.-M. Mårtensson, and S. Svanberg, J. Phys. B **10**, 1971 (1977).
[28]I. Lindgren, Phys. Rev. A **31**, 1273 (1985).
[29]J. S. Deech, P. Hannaford, and G. W. Series, J. Phys. B **7**, 1131 (1974).
[30]A. Gaupp, P. Kuske, and H. J. Andrä, Phys. Rev. A **26**, 3351 (1982).
[31]W. Gawlik, J. Kowalski, R. Neuman, H. B. Wiegman, and K. Winkler, J. Phys. B **12**, 3873 (1979).